

## STUDIES ON SOME ASPECTS OF ZnS NANOCRYSTALS FOR POSSIBLE APPLICATIONS IN ELECTRONICS

Rinki BHADRA<sup>1</sup>, Vidya Nand SINGH<sup>2</sup>, Bodh Raj MEHTA<sup>3</sup>, Pranayee DATTA<sup>4</sup>  
<sup>1,4</sup>*Department of Electronics Science, Gauhati University, Guwahati, Assam-781014, India;*

<sup>2,3</sup>*Thin Film Laboratory, Department of Physics, Indian Institute of Technology Delhi, Hauz Khauz, New Delhi-11016, India*

ZnS nanocrystals are fabricated adopting chemical route. Characterization is done by UV-Visible spectroscopy, X-ray diffraction, Photoluminescence, Energy Dispersive X-ray diffraction and High resolution transmission electron microscopy techniques. Sizes obtained for most of the samples are below exciton Bohr radius for ZnS, which signifies strong confinement. Applications of the fabricated samples as switching element as well as memristors are investigated.

(Received April 12, 2009; accepted April 30, 2009)

*Keywords:* ZnS nanocrystals, X-ray Diffraction, Photoluminescence, memristor

### 1. Introduction

The field of nanotechnology encompasses rapidly emerging technologies based upon the scaling down of existing technology to the next level of precision and miniaturization. Materials in the nanometer scale may exhibit physical properties, distinctively different from that of bulk<sup>1</sup>. Decrease in the particle size gives rise to quantum confinement effect<sup>2</sup>, wherein an increase in the energy gap as well as splitting of the conduction and valence band into discrete energy levels becomes evident. These particles have promising potential applications in nonlinear optics, light emitting materials and optoelectronics.

The II-VI semiconductor ZnS is used in many applications primarily for its luminescent properties. It has a direct band gap of 3.68eV<sup>3</sup> and a small exciton Bohr radius of 2.5 nm<sup>3</sup>. Owing to its wide band gap, it is used in violet and blue regions<sup>4</sup>.

The luminescence of ZnS has been studied by many workers. Kumbhojkar *et al.*<sup>3</sup> have studied the photophysical properties of ZnS nanoclusters. Their work has indicated that mercaptoethanol capped quantum dots show strong band gap luminescence. Nanda *et al.*<sup>5</sup> have studied the photoemission spectroscopic studies of ZnS nanocrystallites. The studies of doped ZnS have also given important results. The luminescence of nanocrystalline ZnS:Pb<sup>2+</sup> has been studied by Bol *et al.*<sup>6</sup>. They have investigated the influence of the size of nanocrystals and the sulphide concentration on the luminescence properties. Bhargava *et al.*<sup>7</sup> have studied the optical properties of Mn doped ZnS nanocrystals and found that Mn doped ZnS nanocrystals can yield both high luminescent efficiencies and lifetime shortening at the same time. Photoluminescence and electroluminescence from copper doped ZnS nanocrystals/polymer composite was studied by Que *et al.*<sup>8</sup>. Borse *et al.*<sup>9</sup> studied the quenching of blue luminescence (at 2.92eV) by Fe and Ni doping.

In 1971, Leon Chua<sup>10</sup> pointed out, for the sake of logical completeness of circuit theory, a fourth passive element in the name of 'memristor' i.e. a resistor with memory, i.e., having hysteresis effect. The I-V characteristics having hysteresis behaviour in many nanoscale electronic

---

\*Corresponding author: rinki12virgo@gmail.com

devices have been observed and reported since 1960. However less attention was given to correlate this observed behaviour with memristive property until very recently Strukov *et al.*<sup>11</sup> concretised the relationship between the observed characteristics and theoretical prediction of Chua. Strukov *et al.*<sup>11</sup> suggested simple model system in which memristance should arise. Their work suggested the existence of memristance in nanometer scale devices.

Bipolar switching has been experimentally observed in various material systems such as organic films<sup>12,13,14,15,16</sup>, chalcogenides<sup>16,17,18,19</sup>, and metal oxides<sup>20,21,16,22</sup>, notably TiO<sub>2</sub><sup>16,23,24,25</sup> and various perovskites<sup>16,26,27,28,29,30</sup>. Typical hysteresis have also been reported by some workers<sup>15,28,29,30,22</sup>. Many of these hysteretic I-V curves show the memristive behaviour. Important applications of memristor include ultradense, semi-non-volatile memories and learning networks that require a synapse-like function<sup>11</sup>.

In the present investigation, we have prepared ZnS nanocrystals embedded in PVA matrix and studied them using various characterization techniques. We have also studied the I-V characteristics of the samples, for investigating the switching and memristive properties of the prepared samples.

## 2. Experimental

### 2.1 Fabrication

#### 2.1.1 Synthesis of sample

Chemical method is followed to prepare undoped ZnS nanocrystals. We have taken poly-vinyl alcohol (PVA) as the matrix. The matrix is prepared by stirring 5gm of PVA in magnetic stirrer at 70°C for 3hours. Aqueous solutions of ZnCl<sub>2</sub> and Na<sub>2</sub>S are used to prepare ZnS nanocrystals. These two solutions are prepared in such a way that the molecular ratio of the chemicals in the solution becomes 1:1. PVA and ZnCl<sub>2</sub> solutions are then mixed in 2:1 volume ratio by stirring the solution at controlled temperature and rotations per minute. To the above solution, Na<sub>2</sub>S solution is added drop by drop to make the solution completely milky. The prepared samples are kept overnight for stabilization and are then caste over glass substrate for characterization. Seven numbers of samples with varying size have been prepared by varying pH, weight of the chemicals, temperature, stirring rate and duration of stirring.

#### 2.1.2 Experimental set-up for current-voltage characteristic

For investigating the switching and memristive properties of the fabricated samples, an electrochemical device is developed and the I-V characteristic is recorded. Two very thin wires of copper/silver are used as electrodes. The wires are fixed over a glass slide. The ends of the wires are kept very close to each other (~ 0.1 cm) and a single tiny drop of the prepared sample is put over it to make a contact. The slide is then dried and connected to the circuit shown in figure 1. DC voltage is then applied and the current is recorded. The circuit in figure 2 is used to check the charge storing property of the device. A small resistor is connected in parallel to discharge the accumulated charge in the sample, while a capacitor is connected in parallel to stabilize the input voltage<sup>31</sup>. After each measurement the power supply was turned off and the device is allowed to discharge for 20 minutes through the resistor.

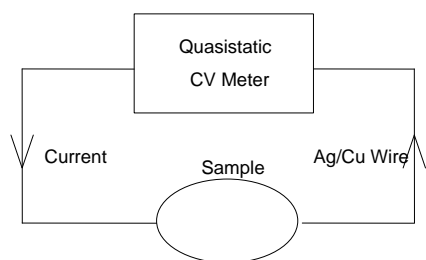


Fig. 1. Experimental set-up to record the I-V characteristic.

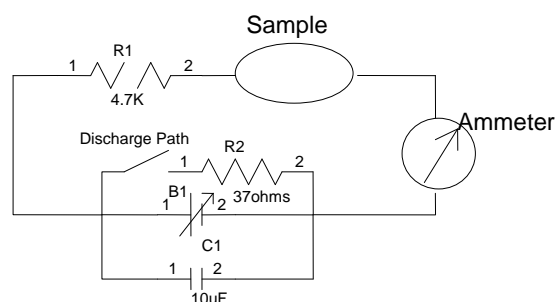


Fig. 2. Experimental set-up to check the charge storing property of the device.

## 2.2 Characterization

Optical absorption studies are made on a HITACHI U-3210 double beam spectrophotometer. X-ray diffraction (XRD) patterns are recorded with an X'Pert Pro X-ray diffractometer, using  $\text{CuK}\alpha$  radiation ( $\lambda = 0.15406 \text{ nm}$ ). The photoluminescence (PL) is recorded in HITACHI F-2500 spectrophotometer. High resolution transmission electron microscopy (HRTEM) as well as Energy dispersive X-ray spectroscopy (EDAX) is carried out on Technai G20-STWIN (at 200kV with point resolution of 1.44Å, line resolution of 2.32Å and having super twin lenses). I-V characteristic is recorded using Keithley 595 Quasistatic CV meter.

## 3. Results and discussion

The characterization results of the samples fabricated are presented below:

### 3.1 Optical Absorption Spectroscopy (OAS)

The absorption spectrum of ZnS is shown in figure 3. The bandgap for the sample is obtained by following the procedure of Tauc<sup>32</sup>. The bandgap obtained is 3.92eV which is blueshifted as compared to the bulk bandgap value<sup>3</sup> and is the evidence for the effect of quantum confinement in the nanoparticles.

However, for two of our samples, we are getting a shoulder at 250 and 227.8nm, respectively, in addition to the main sharp excitonic peak (at 305.4 and 303.8nm respectively) (figure 4 for one sample). The presence of near sharp excitonic peaks in these cases manifests the monodispersity of these samples while the shoulders correspond to a narrow excitonic band. Similar peaks and shoulders are observed by other workers. Chakraborty *et al.*<sup>33</sup> obtained the shoulder at 202-216nm, for ZnS nanoparticles prepared in polymer-surfactant gel matrix, while Kovtyukhova *et al.*<sup>34</sup> reported two absorption peaks at 250 and 300nm for 2nm ZnS nanoparticles prepared in Si film by sol-gel method. Zhao and Fendler<sup>35</sup> observed two absorption peaks at 210 and 325nm for ZnS prepared in LB films with particle size 20 to 200nm.

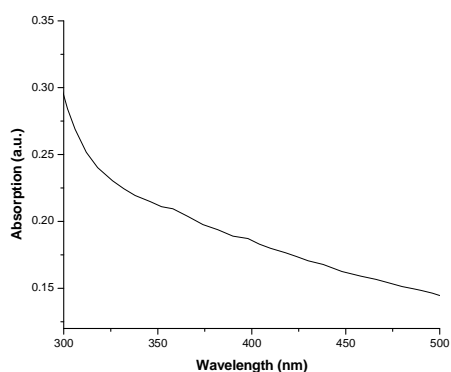


Fig. 3. Absorption spectrum of ZnS nanocrystals

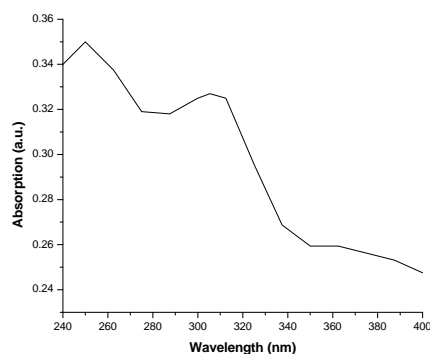


Fig. 4. Absorption spectrum of ZnS nanocrystals

### 3.2 Photoluminescence (PL)

The photoluminescence spectrum of ZnS nanocrystals embedded in PVA is shown in figure 5. The sample is excited at 4.276eV. Two emission peaks are obtained. One narrow peak is at around 3eV and the other broad peak is from 3.4eV to 3.86eV (having shoulders), which is slightly red shifted compared to the optical absorption peak at about 3.92eV and can be attributed to the bandgap luminescence. The peak at  $\sim 3\text{eV}$  (414nm), is the typical luminescence of undoped ZnS nanoparticles and occurs due to the trapped state emission arising from the bulk defects such as vacancies<sup>[36,37]</sup>. In case of ZnS this emission peak is caused due to the transition of electrons from shallow states near the conduction band to the sulphur vacancies present near the valance band<sup>38</sup>. The luminescence spectra of other samples mainly contain a single peak at  $\sim 3\text{eV}$ .

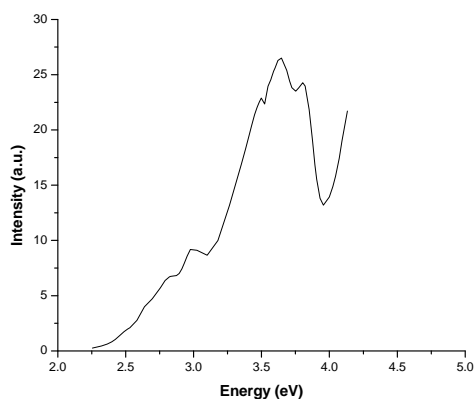


Fig. 5. Photoluminescence spectrum of ZnS nanocrystals embedded in PVA

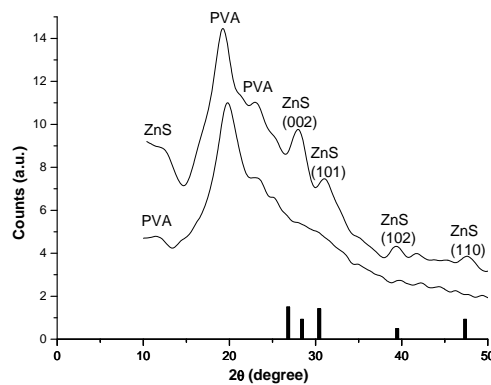


Fig. 6. XRD spectrum of ZnS nanocrystals embedded in PVA (along with the spectrum of PVA)

### 3.3 X-Ray Diffraction (XRD)

Figure 6 shows the XRD spectrum of ZnS nanocrystals embedded in PVA matrix. To detect the peak positions due to the matrix we have taken the XRD of the matrix deposited over a glass slide. The curve shows that the first broad peak is due to the matrix. The other peak positions are showing the sample to be ZnS. The peak positions of the spectrum show the structure to be hexagonal (wurtzite) (JCPDS Card No. 75-1547). The peak positions are at 27.93(002), 30.93(101), 39.44(102) and 47.68(110),  $2\theta$  values. Other samples also show similar XRD pattern. Broadened peak shows the lowering in size. The size has been calculated from half-widths of the diffraction peaks using Debye Scherrer formula<sup>39</sup>, using three peaks and averaging the value. The size obtained is 5.03nm, which shows that we have obtained strong confinement in our sample.

### 3.4 High Resolution Transmission Electron Microscopy (HRTEM)

HRTEM image of ZnS sample is shown in figure 7. The figure shows the polycrystalline nature of the sample with distinct grain boundaries having average crystallite size in the range 5-8nm. The nanoparticles are also seen to be more or less spherical shape with clear lattice fringes showing the well crystallized particles. The d-spacing of planes obtained from HRTEM figure is around 0.28nm, matching fairly well to the (002) plane (JCPDS Card No. 75-1547) and also shown in the XRD spectrum of figure 6. The size is also nearly consistent with the size obtained from XRD observations.

### 3.5 Energy-Dispersive X-Ray Spectroscopy (EDAX)

EDAX chemical characterization curve of undoped ZnS sample is shown in figure 8. We can see the presence of Zn and S. They are present in 54:46 weight% ratios. In addition with Zn and S some other elements are also present. Among them C, Cu and O results from the grid, and Si comes from the detector.

### 3.6 Current-voltage curves

The fabricated samples are tested for application as switch and memristor, using circuit of figures 1 & 2. The room temperature I-V curves show that the conductivity of the samples is low. This nature is to be expected because of non-conducting polymer matrix used to prepare the samples. We can improve the conductivity by using conducting polymer as the matrix.

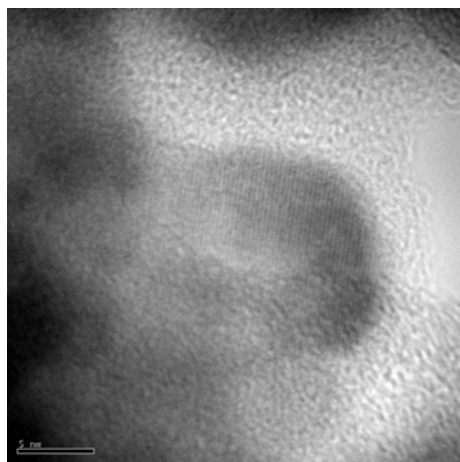


Fig. 7. HRTEM picture of sample S<sub>5</sub>.

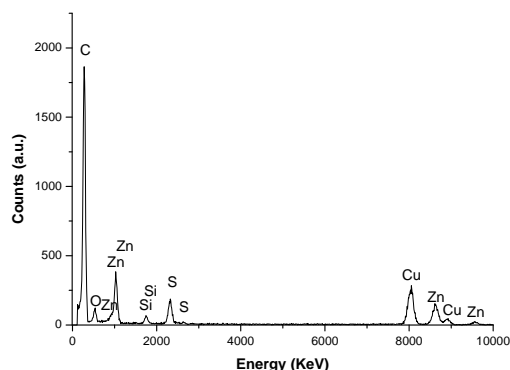


Fig. 8. EDS spectrum of ZnS nanocrystals.

The I-V characteristic of ZnS nanocrystals embedded in PVA matrix is shown in figure 9. The characteristic is studied for increasing and decreasing voltage in the forward as well as reverse direction. The current conduction in the nanocrystals embedded in polymer matrix is governed through tunnelling. Initially as the carriers start tunnelling through the non-conducting polymer matrix the current is very low as it requires a certain minimum voltage depending on the thickness and property of the matrix in between. After around 1V the current rises almost linearly with rise in voltage. After reaching a certain value there is saturation in the current suggesting that the tunnelling of charge carriers is saturated. This saturation is more prominent in the negative voltage region. The current then goes back to zero as we start decreasing it towards zero. So, hysteresis is observed in our sample. The figure also shows asymmetry in the characteristics. This asymmetry can be ascribed to the Schottky contact at the interface between the nanocrystallite (semiconductor) sample and the metal electrode<sup>29</sup>. The important characteristic of I-V curve, however, is hysteresis

between increasing and decreasing voltage, and that behaviour is irrelevant to the existence of asymmetry.

Strukov *et al.*<sup>11</sup> has shown that for a memristor any symmetrical alternating current voltage bias results in double-loop I-V hysteresis that collapses to a straight line for high frequencies. Multiple continuous states will also be obtained if there is any sort of asymmetry in the applied bias. Thus for dc voltages, the I-V characteristics must exhibit hysteresis and for successive observations (repeated immediately), multiple loops may be expected. To check this phenomenon we have recorded the I-V curve for two cycles of voltage repeated immediately and have obtained multiple loops which are different from each other (figure 10). It shows that the resistance of our sample to the electricity flow depends on the amount of charge that has recently passed through it. It works as its internal structure rearranges as the charge flows<sup>40</sup>. The similar behaviour is speculated for memristor, i.e., resistor with memory. To prove this point we can check the I-V curve of the sample after discharging the sample for about 20min, through the circuit given in figure 2. The I-V curve obtained is given in figure 11. We can observe that the curve is almost similar to the one obtained before discharging.

Alongwith the hysteresis, we have also obtained binary switching property (for sample having different growth parameters, figure 12) which is similar to that modelled by Strukov *et al.*<sup>11</sup>. In this curve the current starts decreasing after attaining its maximum value and the saturation region is very narrow. The curve clearly shows the switching property. Figure 13 shows another sample with I-V behaviour resembling that of voltage regulator.

An interesting behaviour is obtained in case the two electrodes are of two different metals (silver and copper). We obtained a gradual decrease of current with time at fixed applied voltage as shown in figure 14. The explanation of this behaviour needs further investigation.

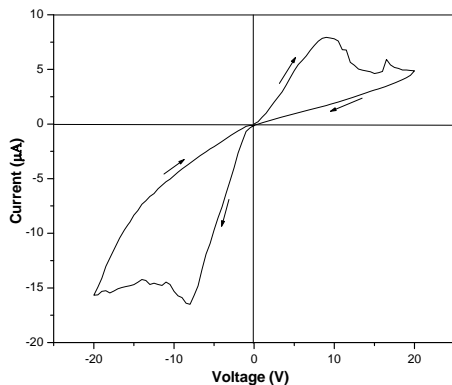


Fig. 9. I-V curve of ZnS nanocrystal embedded in PVA.

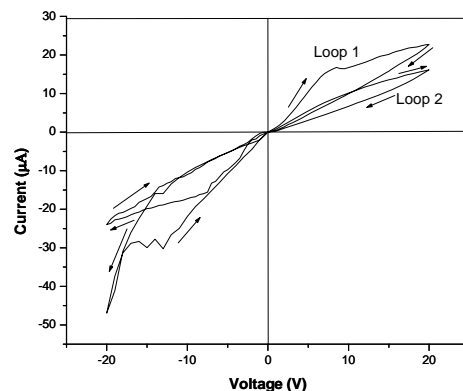


Fig. 10. I-V curve obtained for consecutive voltage cycles.

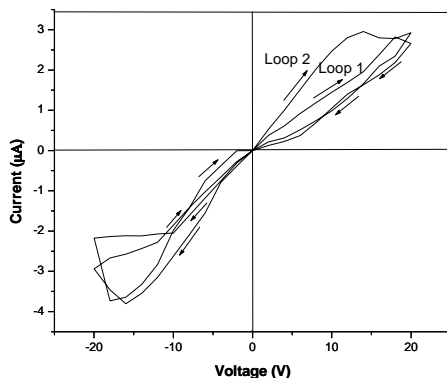


Fig. 11. I-V curve tested for after discharging the sample for 20 minutes.

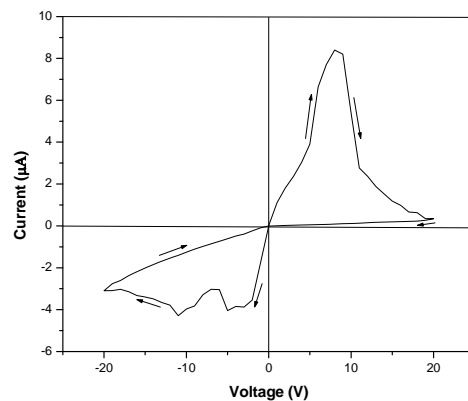


Fig. 12. I-V curve showing the switching property

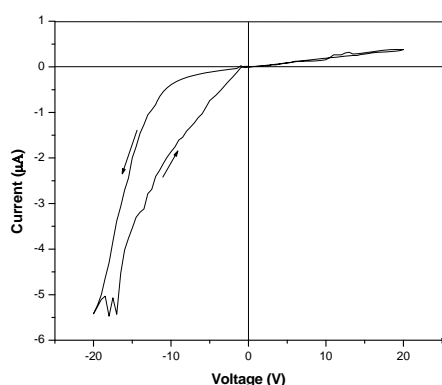


Fig. 13. I-V curve showing the voltage regulator behaviour.

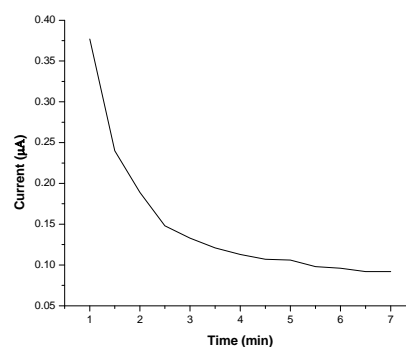


Fig. 14. Decrease in current with time for (at  $V = 10V$ ).

#### 4. Conclusions

- Optical absorption (UV-Vis spectroscopy) spectrum confirms quantum confinement for the prepared samples.
- PL emission is obtained in the range  $\sim 3$  to  $4eV$ . The luminescence at around  $3eV$  is attributed to the sulphur vacancies.
- The size of the synthesized ZnS nanoparticles is found to be smaller than excitonic Bohr radius signifying strong confinement.
- UV-Vis spectroscopy, XRD, PL, EDAX and HRTEM observation shows that we have successfully fabricated ZnS nanocrystals embedded in PVA matrix by chemical method.
- The synthesized samples have the basic property of memristor viz. binary switching property and the hysteresis property for both voltage polarities as well as one voltage polarity. Thus the two terminal devices fabricated from the ZnS nanocrystals embedded in PVA has the potential for application as electronic switch and memristor.

#### Acknowledgement

The authors would like to acknowledge the Department of Chemistry, Gauhati University for spectrophotometer observations, Dept. of Instrumentation and USIC, Gauhati University for XRD observations and the Department of Science and Technology (DST), for the computer lab facility provided in the Department of Electronics Science, Gauhati University.

#### References

- [1] G. Cao, Nanostructures and Nanomaterials: Synthesis, Properties and Applications, Imperial College Press, London (2004).
- [2] L.E. Brus, J. Phys. Chem. **90**, 2555 (1986).
- [3] N. Kumbhojkar, V. V. Nikesh, A. Kshirsagar, S. Mahamuni, J. Appl. Phys. **88**, 6260 (2000).
- [4] N. Karar, F. Singh, B.R. Mehta, J. Appl. Phys. **95**, 656 (2004).
- [5] J. Nanda, D.D. Sarma, J. Appl. Phys. **90**, 2504 (2001).
- [6] A.A. Bol, and A. Meijerink, Phys. Chem. Chem. Phys. **3**, 2105 (2001).
- [7] R.N. Bhargava, D. Gallagher, X. Hong, A. Nurmikko, Phys. Rev. Lett. **72**, 416 (1994).
- [8] W. Que, Y. Zhou, Y.L. Lam, Y.C. Chan, C.H. Kam, B. Liu, L.M. Gan, C.H. Chew, G.Q. Xu, S.J. Chua, S.J. Xu, F.V.C. Mendis, Appl. Phys. Lett. **73**, 2727 (1998).
- [9] P.H. Borse, N. Deshmukh, R.F. Shinde, S.K. Date, S.K. Kulkarni, J. Mat. Sc. **34**, 6087 (1999).
- [10] L.O. Chua, IEEE Trans. circuit theory. **18**, 507 (1971).

- [11] D.B. Strukov, G.S. Snider, D.R. Stewart, R.S. Williams, *Nature*. **453**, 80 (2008).
- [12] J.C. Scottand, L.D. Bozano, *Adv. Mater.* **19**, 1452 (2007).
- [13] C.P. Collier, G. Mattersteig, E.W. Wong, Y. Luo, K. Beverly, J. Sampaio, F.M. Raimo, J.F. Stoddart, J.R. Heath, *Science*. **289**, 1172 (2000).
- [14] N. B. Zhitenev, A. Sidorenko, D.M. Tennant, R.A. Cirelli, *Nature Nanotechnol.* **2**, 237 (2007).
- [15] J.H.A. Smits, S.C.J. Meskers, R.A.J. Janssen, A.W. Marsman, D.M. de Leeuw, *Adv. Mater.* **17**, 1169 (2005).
- [16] Q.X. Lai, Z.H. Zhu, Y. Chen, S. Patil, F. Wudl, *Appl. Phys. Lett.* **88**, 133515 (2006).
- [17] K. Terabe, T. Hasegawa, T. Nakayama, M. Aono, *Nature*. **433**, 47 (2005).
- [18] M.N. Kozicki, M. Park, M. Mitkova, *IEEE Trans. Nanotechnol.* **4**, 331 (2005).
- [19] S. Dietrich, M. Angerbauer, M. Ivanov, D. Gogl, H. Hoenigschmid, M. Kund, C. Liaw, M. Markert, R. Symanczyk, L. Altimime, S. Bournat, G. Mueller, *IEEE J. Solid State Circuits.* **42**, 839 (2007).
- [20] M.T. Hickmott, *J. Appl. Phys.* **33**, 2669 (1962).
- [21] G. Dearnaley, A.M. Stoneham, D.V. Morgan, *Rep. Prog. Phys.* **33**, 1129 (1970).
- [22] C.A. Richter, D.R. Stewart, D.A.A. Ohlberg, R.S. Williams, *Appl. Phys. Mater. Sci. Process.* **80**, 1355 (2005).
- [23] J.R. Jameson, Y. Fukuzumi, Z. Wang, P. Griffin, K. Tsunoda, G.I. Meijer, Y. Nishi, *Appl. Phys. Lett.* **91**, 112101 (2007).
- [24] D.S. Jeong, H. Schroeder, R. Waser, *Electrochem. Solid State Lett.* **10**, G51 (2007).
- [25] D.R. Stewart, D.A.A. Ohlberg, P.A. Beck, Y. Chen, R.S. Williams, J.O. Jeppesen, K.A. Nielsen, J.F. Stoddart, *Nano Lett.* **4**, 133 (2004).
- [26] A. Beck, J.G. Bednorz, C. Gerber, C. Rossel, D. Widmer, *Appl. Phys. Lett.* **77**, 139 (2000).
- [27] K. Szot, W. Speier, G. Bihlmayer, R. Waser, *Nature Mater.* **5**, 312 (2006).
- [28] A. Sawa, T. Fujii, M. Kawasaki, Y. Tokura, *Appl. Phys. Lett.* **88**, 232112 (2006).
- [29] M. Hamaguchi, K. Aoyama, S. Asanuma, Y. Uesu, T. Katsufuji, *Appl. Phys. Lett.* **88**, 142508 (2006).
- [30] R. Oligschlaeger, R. Waser, R. Meyer, S. Karthaus, R. Dittmann, *Appl. Phys. Lett.* **88**, 042901 (2006).
- [31] S. Jafri, S. Promnimit, C. Thanachayanont, J. Dutta, Available at <http://www.nano.ait.ac.th/Download/AIT%20Papers/2007/Jafri%20al,%20USMCA%202006%20Phuket%20Nov.pdf>
- [32,33,34,35] I. Chakraborty and S.P. Moulik, *J. Dispersion Sc. & Tech.* **25**, 849 (2004) (and the references therein).
- [36] H. Li, W.Y. Shih, W.H. Shih, *Nanotech.* **18**, 205604 (2007).
- [37] W. Chen, Z. Wang, Z. Lin, L. Lin, *J. Appl. Phys.* **82**, 3111 (1997).
- [38] H.C. Warada, S.C. Ghosha, B. Hemtanona, C. Thanachayanontb, J. Duttaa, *Sci. Tech. Adv. Mat.* **6**, 296 (2005).
- [39] S.Y. Chang, L. Liu, A. Asher, *J. Am. Chem. Soc.* **116**, 6739 (1994).
- [40] R.V. Noorden, *Chemistry world.* **5** (2008), Available at <http://www.rsc.org/chemistryworld/News/2008/April/30040803.asp>